Computational Study of the Adsorption Energetics and Vibrational Wavenumbers of NH_3 Adsorbed on the Ni(111) Surface

Theo Kurten,[†] Małgorzata Biczysko,[†,‡] Timo Rajamäki,[†,§] Kari Laasonen,[||] and Lauri Halonen*[,†]

Laboratory of Physical Chemistry, P.O. Box 55 (A.I. Virtasen aukio 1), FIN-00014 University of Helsinki, Finland, and Department of Chemistry, P.O. Box 3000, FIN-90014 University of Oulu, Finland

Received: December 13, 2004; In Final Form: February 28, 2005

The structure and stabilities of NH_3 adsorbed on different sites of a Ni(111) surface are compared based on density functional, plane-waves calculations within a periodic framework. The surface has been modeled by 4- and 5-layer slabs with 2×2 and 3×3 unit cells. Calculated results are in good agreement with available experimental data, confirming the atop adsorption site to be the most favorable, with no preferred azimuthal orientation for the H atoms. For NH_3 adsorbed at the atop site, the one-dimensional potential energy profiles along the N−H and N−Ni bonds and the coupling between adjacent N−H bond oscillators have been calculated and fitted to an analytical expression using an accurate anharmonic potential model. Variational calculations have been performed to obtain frequencies for the N−H and N−Ni stretching vibrations and N−H stretching line widths. The model for calculating line widths has also been tested with CO adsorbed at the hcp hollow of the Ni(111) surface.

1. Introduction

There have been many studies of small molecules adsorbed on ideal metal surfaces in ultrahigh-vacuum (UHV) conditions (see ref 1 for extensive references to original work in this field). Many of these contributions have focused on CO, and much less is known of hydrogen-containing molecules such as NH_3 or H_2O. Interactions of water with metal surfaces are important, but ammonia also has several significant surface applications. These include the Haber−Bosch ammonia synthesis.[2] Another issue of interest is the importance of vibrational excitation for molecular reactions on catalytic metallic surfaces.[3,4]

There are some experimental[5−15] but few theoretical[16,17] studies of NH_3 adsorbed on a Ni(111) surface. It has been found that the α-type monolayer of ammonia is observed at coverages ≤ 0.25 monolayers (ML),[10] with an even lower saturation coverage of 0.14 ML postulated based on the low-energy diffraction [LEED] measurements.[13] At higher coverages, the β-type NH_3/Ni(111) layer has been formed by hydrogen bonding of the second ammonia layer to α-NH_3/Ni(111).[11] Early experiments performed in the 1980s[5−11] have shown that at low coverages α-NH_3 adsorbs molecularly, with the nitrogen lone pair facing the surface, and with the 3-fold rotational axis normal to the surface. However, the preferred adsorption site has not been determined unequivocally. There has also been controversy concerning the azimuthal orientation of ammonia molecules, as an electron-simulated-desorption ion angular distribution (ESDIAD) study[6,7] has postulated an azimuthal disorder of NH_3 molecules on a clean Ni(111) surface, but the angle-resolved photoemission spectroscopy (ARPS)[9] has ruled out freely rotating NH_3 molecules under the experimental conditions. The latter result has, however, subsequently been attributed to small amounts of surface contaminants.[6,8] These early experiments have mostly suggested a 3-fold site (face-centered-cubic, or fcc, hollow) for NH_3 adsorption on Ni(111). For example, Fisher and Mitchell[11] have suggested in 1983 that ammonia adsorbs at the fcc hollow site, based on the absence of an N−Ni stretching vibration in the electron energy loss (EEL) spectra. It was postulated that adsorption at the fcc hollow site could affect the transition dipole moment of the N−Ni vibration. Available theoretical studies have generally been consistent with adsorption at the fcc hollow site. In 1990, Chattopadhyay et al. performed ab initio calculations[17] with the Ni(111) lattice being modeled by a 28-atom, 3-layer cluster, showing the atop, 3-fold fcc and bridge sites to be of comparable stability. However, in 1992, the adsorption of NH_3 on Ni(111) was investigated by photoelectron diffraction,[15] and the atop adsorption site was determined to be the most favorable. In the same study, the N−Ni bond length was measured to be 1.97 ± 0.3 Å.

The purpose of this paper is a theoretical reinvestigation of NH_3 adsorption on Ni(111), as at present there is no theoretical work consistent with all available experimental data. Our study is performed within a periodic framework, which is more suitable than the cluster model for the treatment of surfaces. The structure and stabilities of ammonia adsorbed on the Ni-(111) surface at different adsorption sites are calculated and compared to existing experimental and theoretical data. Moreover, the calculated potential surfaces are used to perform variational vibrational calculations for the ammonia molecule adsorbed at the atop site. Our vibrational analysis takes into account anharmonicity, and it is accordingly more thorough and accurate than what is normally performed in surface studies.

2. Computational Details

2.1. Electronic Structure Calculations. All electronic structure calculations were performed within a periodic frame-

* To whom correspondence should be addressed. Fax: +358 9 19150279. E-mail: lauri.halonen@helsinki.fi.
[†] University of Helsinki.
[‡] Current address: Departamento de Quimica, Universidade de Coimbra, 3004−535 Coimbra, Portugal.
[§] Current address: Temet Instruments Ltd., Pulttitie 8, FIN-00880 Helsinki, Finland.
[||] University of Oulu.

10.1021/jp044326w CCC: $30.25
Published on Web 04/19/2005

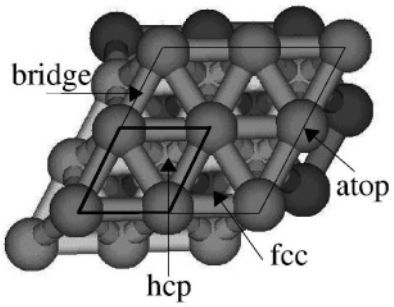

Figure 1. Adsorption sites on the Ni(111) surface. The 2 × 2 unit cell is enclosed by the thick line and the 3 × 3 unit cell by the thin line.

work making use of density functional theory (DFT) with the plane-wave pseudopotential formalism, using the Vienna Ab Initio Simulation Package (VASP).[18] The surface was modeled by 4- and 5-layer slabs, separated by 10 Å of vacuum, with 2 × 2 and 3 × 3 unit cells, using a PW91 generalized gradient approach (GGA), ultrasoft pseudopotentials and a 437 eV energy cutoff. All results are based on spin-restricted calculations. The effect of the spin polarization was tested in the case of the molecular adsorption energies. The theoretical equilibrium lattice constant[19] (3.53 Å) was used in all surface calculations. One adsorbant (ammonia) molecule per unit cell was placed on one side of the slab. See Figure 1 for an illustration of the unit cells.

For the studies of NH_3 adsorption at different surface sites, the 5 × 5 × 1 *k*-point mesh reduced using the symmetry of the unit cell (5 unequivalent *k*-points) was used. The adsorbant structure was fully optimized, allowing the two uppermost surface layers to relax.

For the 3 × 3 unit cells, an ionic convergence limit of 10^{-3} eV and an electronic convergence limit of 10^{-4} eV were used. For all calculations with 2 × 2 unit cells, the electronic energy was converged to 10^{-4} eV, and the positions of the atoms that were allowed to relax were optimized until all forces were smaller than 0.005 eV/Å^2. The calculation was stopped after 100 ionic steps if these ionic convergence criteria were not met (this was the case for the less favorable adsorption sites). In such cases, the energies were always converged to at least 3 × 10^{-4} eV.

For the accurate calculations of N−H potential energy profiles, the equilibrium geometries of both free ammonia and ammonia adsorbed at the atop site were first optimized to high numerical accuracy (using the convergence criteria given above) with the surface modeled by a 2 × 2 unit cell, a 5-layer slab and using the hexagonally symmetric 5 × 5 × 1 *k*-points mesh (13 unequivalent *k*-points). It was found to be important to use a nonreduced hexagonally symmetric *k*-point mesh for NH_3 geometries distorted from C_{3v} symmetry. The reduced mesh led to serious errors; for example, the three N−H bond oscillator potential energy curves were different. The errors were probably due to the NH_3 adsorbant breaking the original symmetry of the surface. Even though the system was still C_{3v} symmetric after adsorption, only one of the four Ni atoms now constituted a symmetry center.

2.2. Vibrational Calculations. Many studies on surface adsorbates treat vibrational motion using the harmonic approximation. When information beyond the harmonic model is desired, vibrational spectra are usually calculated from ab initio molecular dynamics data.[20,21] We chose to pursue a different route in this work. We mapped a local potential energy hypersurface for NH_3 adsorbed on Ni(111) by several grid points and fitted the data to a more realistic analytic representation. This is a common approach in accurate vibrational calculations for isolated molecules, but it is more seldom used in surface studies. See, for example, ref 22, where an unprecedented accuracy of 1 cm^{-1} between experiments and calculations is achieved for ammonia.

The one-dimensional potential energy curve along the N−H stretching coordinate was mapped at 16 points by displacing one hydrogen atom along the direction of the N−H bond, keeping all other atomic positions fixed. For ammonia bound to the nickel surface, the N−Ni potential energy curve was also calculated. This was done by displacing the ammonia molecule along the N−Ni bond, keeping all other atomic positions fixed. The effect of keeping the NH_3 intermolecular bond lengths and angles fixed but relaxing the top nickel layer was also investigated. A total of 16 data points were calculated both for the fixed and relaxed Ni surfaces.

A simple potential energy model that adequately reproduces the asymptotic behavior of real chemical bonds is the Morse function[23]

$$V(\Delta r) = D_e(1 - e^{-a\Delta r})^2 \quad (1)$$

where a is the Morse steepness parameter, D_e is the dissociation energy and $\Delta r = r - r_e$ is the displacement from the equilibrium bond length r_e. In this study, a simple local mode model, with only the stretching vibrations of ammonia and the N−Ni stretch considered, has been implemented using both the Morse potential and its high-order generalization. It should be noted that, although the ab initio calculations are performed in a periodic framework, the potential energy models used do not explicitly take periodic interactions into account.

For the N−H vibrations, the calculated ab initio energies were first fitted to a normal Morse potential (eq 1) in order to obtain a value for the shape parameter a. (All fits in this work were done using the least-squares method.) This value of a was then used to fit the data to an eigth-order Chebyshev polynomial in the Morse coordinate $y = 1 - e^{-a\Delta r}$ to make the fit more stable[24]

$$V(y) = \sum_{n=0}^{8} D_n C_n(y) \quad (2)$$

where C_n is the nth order Chebyshev polynomial and D_0, ..., D_8 are adjustable parameters.

The potential energy coupling between two N−H-oscillators was estimated by calculating 11 data points in which two hydrogen atoms were simultaneously displaced from their equilibrium positions. Since the effect of the coupling was small compared to the total vibrational energy, the coefficient of the coupling term was optimized separately, using the equation

$$V(\text{coupling}) = V(\Delta r_1,\Delta r_2) - V(\Delta r_1,0) - V(0,\Delta r_2) = f\Delta r_1\Delta r_2 \quad (3)$$

where Δr_i is the linear displacement of the ith hydrogen atom. Linear displacements were used instead of Morse coordinates as the fit was observed to be better with eq 3.

The N−Ni vibrational energies were fitted to the standard Morse potential given in eq 1, as precise vibrational wavenumbers were difficult to compute due to reasons that will be discussed in section 3.3.

The stretching vibrational variational calculations are based on a simple local-mode Hamiltonian where the anharmonic N−H bond oscillators are coupled by bilinear harmonic potential energy (eq 3) and kinetic energy terms.[25] The Ni−N oscillator

is assumed to be decoupled from the N−H oscillators in the variational calculations. The eigenvalues have been calculated using symmetrized bond product Morse oscillator wave functions for the N−H bond oscillators as described in ref 26 for CH_3D-type molecules. The Morse basis functions in the case of both N−H and Ni−N oscillators are chosen to be consistent with the appropriate potential energy parameters a and D_e. The matrix elements of the kinetic and potential energy coupling terms have been computed with analytic formulas,[27] and the matrix elements of the potential energy term in eq 2 have been obtained with a 24-point Gauss-Laguerre numerical integrations as explained in ref 3. All stretching states up to 8 excited vibrational quanta in both N−H and Ni−N oscillators have been included. Test calculations show that all reported eigenvalues are converged better than 0.01 cm^{-1}.

The coupling between the N−H and N−Ni oscillators was also investigated. However, the 16 coupling data points calculated could not be fitted reliably to a bilinear term such as that presented in eq 3. Instead, this coupling was treated by estimating the line width of the N−H stretching peaks due to the N−Ni vibration.

Our treatment of the broadening of the N−H stretching vibrational bands differs from earlier approaches[28−30] in the sense that we have not explicitly specified its mechanism, though our frozen-lattice approach rules out both vibrational dephasing and coupling to surface phonons. Instead, we used our potential energy surface to estimate the magnitude by which the N−Ni distance affects the N−H stretching wavenumbers. As our calculations were performed on a perfect surface with a homogeneous distribution of ammonia molecules, the computed linewidhts presented here correspond to what is normally defined (e.g., by Hoffmann in ref 30) as homogeneous broadening.

3. Results and Discussion.

3.1. Adsorption of NH_3 at the Ni(111) Surface. The adsorption energy and geometry of ammonia on Ni(111) were calculated at four different sites: atop, bridge, fcc hollow and hcp (hexagonal close packed) hollow, as shown in Figure 1. The calculations were carried out using 2 × 2 and 3 × 3 unit cells with up to 5 Ni layers. The two uppermost Ni layers were allowed to relax in the 2 × 2 cell, and the uppermost Ni layer was allowed to relax in the 3 × 3 cell. The convergence of the results with respect to the number of Ni layers and k-points was tested. Increasing the number of k-points from 5 × 5 × 1 to 7 × 7 × 1 changed the absolute adsorption energies by less than 0.48 kcal/mol, and the relative stabilities of the different sites by less than 3.0%. The effect of spin polarization was also tested. Using the spin polarized version of the PW91 functional almost doubled the calculation time, but affected the relative stabilities of the adsorption sites by less than 0.9 kcal/mol, and did not change the order of stability of the sites. Thus, the less expensive spin-restricted calculations are accurate enough to describe the Ni−ammonia interactions, but in general, the spin polarization calculations are preferred since nickel is a magnetic material.

The geometric parameters and adsorption energies of NH_3 bound to different sites of Ni(111) are listed in Table 1 along with available experimental data.[13,15] Ab initio results with the Ni(111) surface modeled as a 28-atom cluster[17] are also given. The periodic calculations performed using 2 × 2 and 3 × 3 unit cells correspond to ammonia coverages of 0.25 and 0.11 ML, respectively, both in the range of experimentally postulated saturation coverages.[10,13] The obtained results show that although the absolute adsorption energies for the calculations using 2 × 2 and 3 × 3 cells differ significantly, the relative stabilities of the adsorption sites (defined as the difference between the adsorption energy at that site and at the atop site) are close, with a maximum deviation of 1.1 kcal/mol. The distances from N to the closest Ni atom on the surface [r(N−Ni)] vary by less than 0.1 Å. The maximum difference for distances perpendicular to the surface is 0.12 Å. The slightly smaller distances in the 3 × 3 cells correspond to the greater adsorption energies, except for the bridge site. The 3−6 kcal/mol overall decrease in adsorption energy values in going from the 3 × 3 cell to the 2 × 2 cell indicates a repulsive adsorbate−adsorbate interaction. Such interactions are common between molecules adsorbed on metal surfaces.[31] The magnitude of this effect was investigated by placing two ammonia molecules on adjacent atop sites in the same 3 × 3 cell and calculating the adsorption energy. After relaxation of the ammonia molecules and the top Ni layer, the shortest distance between two nitrogen atoms was 3.08 Å, as opposed to 4.99 Å in the 2 × 2 cell and 7.49 Å in the normal 3 × 3 cell. Correspondingly, the adsorption energy had decreased to 12.43 kcal/mol, as opposed to 15.61 kcal/mol in the 2 × 2 cell and 20.35 kcal/mol in the normal 3 × 3 cell. As the magnitude of the repulsion was large, its origin was further investigated by calculating the direct lateral interaction between the adsorbants. This was done by computing the energy for ammonia molecules frozen in configurations corresponding to the three adsorption patterns described above, but without any surface atoms, and subtracting the energy calculated for an isolated ammonia molecule.

TABLE 1: Adsorption of NH_3 on Different Sites of the Ni(111) Surface[a]

	source	r(N-surface) (Å)	r(N−Ni) (Å)	E_{ads} (kcal/mol)	ΔE (kcal/mol)
atop	2 × 2[b]	2.010	2.010	15.61	0.00
	3 × 3[c]	1.999	1.999	20.35	0.00
	cluster[d]	2.12	2.12	19.4	0.0
bridge	2 × 2[b]	2.127	2.456	4.53	−11.08/ −10.61[e]
	3 × 3[c]	2.145	2.499	8.88	−11.47
	cluster[d]	2.44	2.74	17.3	−2.1
hcp hollow	2 × 2[b]	2.296	2.710	3.13	−12.48/ −11.66[e]
	3 × 3[c]	2.174	2.624	6.81	−13.54
	cluster[d]	2.38	2.78	18.4	−1.0
fcc hollow	2 × 2[b]	2.255	2.676	3.01	−12.59/ −11.74[e]
	3 × 3[c]	2.149	2.602	7.14	−13.21
	cluster[d]	2.37	2.77	13.8	−5.6
exp.			1.97[f]	17[g]	

[a] The relative stabilities ΔE calculated as difference to the atop site. [b] Ni surface modeled by a 2 × 2 unit cell, 5-layer slab with the two uppermost layers allowed to relax, this work. [c] Ni surface modeled by a 3 × 3 unit cell, 4-layer slab with the uppermost layer allowed to relax, this work. [d] Ni surface modeled by a 28-atom cluster. ref 17. [e] Spin−polarized calculations. [f] Reference 15. [g] Reference 13.

For the configuration corresponding to the 2 × 2 cell, the magnitude of the direct lateral repulsion was 0.87 kcal/mol. The values corresponding to the 3 × 3 cell were 0.42 and 2.40 kcal/mol, for one and two ammonia molecules per cell, respectively. Thus, though the direct lateral repulsion increases with decreasing intermolecular distance, lateral interactions alone do not explain the large differences between the calculated adsorption energies. Therefore, the observed repulsive interaction is surface-mediated.

Both the 2 × 2 and 3 × 3 cell calculations predict that the adsorption energy is largest and the N−Ni distance smallest at the atop site. The bridge, hcp hollow, and fcc hollow sites

possess similar adsorption energies and are all predicted to be less stable than the atop site by over 10 kcal/mol. Correspondingly, the minimum N−Ni distances at the less stable sites are predicted to be between 0.45 and 0.7 Å longer than at the atop site. The periodic calculations at the atop site reproduce the experimental N−Ni bond length and adsorption energy well. For both the 3×3 and 2×2 unit cells, the adsorption energies are within 3 kcal/mol and the bond lengths within 0.04 Å of the experimental values. The exact error of adsorption energy is not stated[13] and bond lengths are determined with an accuracy of ±0.03 Å.[15] As precise experimental NH_3 coverages are also unknown, the agreement between the experiment and theory is good. The barrier for rotation of ammonia along its C_3 axis perpendicular to the surface has been calculated for the 2×2 unit cell and the atop adsorption site at 15° intervals. The calculated rotational barrier is less than 30 cm^{-1} and is too small to cause any azimuthally preferred orientation. This result is in agreement with experimental studies.[6−9] Stretching one N−H bond by 0.175 Å (roughly corresponding to one quantum of vibrational exitation) increases the rotational barrier by less than 5 cm^{-1}.

This work shows differences to the previous computational studies for the NH_3/Ni(111) system, as the atop site is over 10 kcal/mol more favorable than the other sites. This is in agreement with the most recent experiments.[15] The only other theoretical calculations available, which used a cluster model for the Ni surface,[17] also predicted the atop site to be the most stable one, but the fcc hollow and bridge sites possessed a similar stability (within 2 kcal/mol). Periodic surface models have been expected to be better than cluster models for calculating properties of ideal surfaces. Cluster models, unlike periodic models, cannot simulate true delocalized surface and bulk electronic states. Also, almost all atoms in a cluster are on the surface, which has a large effect on the electronic states. Nevertheless, the cluster calculations by Chattopadhyay et al.[17] are thorough. They modeled the surface with a 28-atom cluster embedded to a field caused by ideal Ni atoms. The cluster and ammonia molecule were studied by CI methods, but an unusual pseudopotential for Ni was used. Our computational approaches are different. Still, the large differences between published and our results are suprising. The better correspondence between our calculations and the experimental values may be due to the inherent differences between the two methods.

3.2. Calculated Energy Profiles for NH_3 on atop Ni(111). The potential energy profiles along the N−H stretch coordinate calculated for free NH_3 and NH_3 adsorbed at the atop site of Ni(111) presented in Figure 2 show a significant lowering (about 13 000 cm^{-1}) of the dissociation energy upon adsorption on the surface. As already mentioned, the calculated potentials have been fitted to a model that does not explicitly account for the periodicity of the surface. However, as seen in Figure 2, even at the furthest grid point used in the fit (corresponding to an 1.0 Å stretch of the N−H bond), no direct interaction between adjacent ammonia molecules can be observed. This is not surprising, as the closest distance between H atoms belonging to adjacent ammonia molecules was over 2.74 Å at that grid point. This probably rules out any significant direct interactions between hydrogen atoms.

The shape of the N−H potential curve depends on the N−Ni distance. The N−H bond becomes weaker as ammonia approaches the surface, causing the vibrational wavenumbers to redshift. A 5-point N−H potential curve was calculated at five different N−Ni bond lengths including the equilibrium position. Each set of points was fitted to a Morse potential (eq 1), and

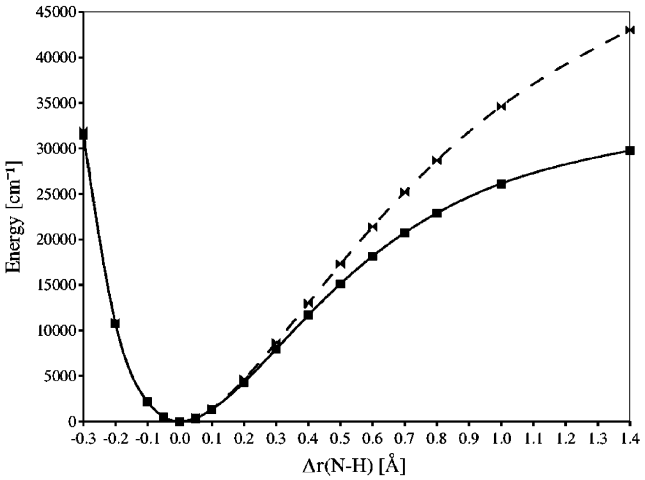

Figure 2. One-dimensional potential energy profile along the N−H bond for NH_3 adsorbed on the atop site of Ni(111) (solid line) and for a free molecule (dashed line), see text for details.

approximate N−H stretching vibrational wavenumbers were calculated for each parameter set using the vibrational variational program. For the N−Ni equilibrium distance, the difference between the fundamental vibrational transition wavenumbers obtained by using eq 1 and a 5-point fit differed from the more accurate ones obtained by using eq 2 and a 16-point fit by less than 10 cm^{-1}.

The variation of the N−H potential energy profile with the number of Ni layers was investigated by calculating a 5-point potential energy curve with 3, 4, 5, and 6 Ni layers, with the two uppermost layers kept in the equilibrium configuration obtained by relaxation for the 5-layer case. It was assumed that recalculating the equilibrium configuration for each slab thickness would not be cost-effective. It was found that the profile changed little as the number of Ni layers was varied from 3 to 6. The effect of changing the thickness of the Ni slab on the N−H vibrational wavenumbers was investigated by fitting the 5-point potential energy curves to the Morse potential (eq 1), and using the obtained coefficients in the variational program. The wavenumbers of the fundamental stretching transitions differed by less than 0.13%, and the absolute vibrational energies differed by less than 2.7%, as the number of Ni layers was varied from 3 to 6. Thus, we concluded that a 5-layer slab is sufficiently thick to model the effect of a real Ni surface on adsorbant molecules.

3.3. Vibrational Wavenumbers for NH_3 on atop Ni(111). The parameters obtained from the fit of the N−H potential surface to the standard Morse potential and the Chebyshev polynomial expansion are given in Table 2, whereas the root-mean-square errors and maximum deviations of both fits are listed in Table 3. We have given some extra digits in Table 2 in order to facilitate repeating of the calculations. The N−Ni Morse parameters for both the fixed-surface and the relaxed-surface potential curves are given in Table 2. It can be seen from Table 3 that a Morse potential is not adequate for the N−H stretching part of the potential energy surface if spectroscopic accuracy is required. Therefore, an analytical representation of the potential energy function in terms of Chebyshev polynomials was used to obtain the wavenumbers of the fundamental and overtone N−H stretching transitions by variational vibrational calculations. It should be noted that, although the Chebyshev polynomial series used converges slowly, the quality of the fit is more than sufficient for our purposes.

The calculated anharmonic vibrational wavenumbers for the N−H and N−Ni stretching modes and the ν(N−H) full width

TABLE 2: Numerical Values of Parameters from the Fit of N−H and N−Ni Potential Energy Points to the Morse Function and to the Chebyshev Polynomial Expansion in the Morse Co-Ordinate

	N−H (atop)	N−H (free)
a(N−H)/Å^{-1}	2.27964	2.0223
D_e(N−H)/cm^{-1}	32518.32	44290.16
f/cm^{-1}Å^{2} [a]	−2117.56	−2405.91
r_e(N−H)/Å [b]	1.0231	1.0205
D_0/cm^{-1}	16187.4	23518.0
D_1/cm^{-1}	−36.01	−113.89
D_2/cm^{-1}	16203.1	24771.2
D_3/cm^{-1}	−136.99	185.83
D_4/cm^{-1}	29.06	1621.82
D_5/cm^{-1}	−168.44	80.84
D_6/cm^{-1}	37.04	442.87
D_7/cm^{-1}	−46.77	−41.97
D_8/cm^{-1}	23.77	74.28
a(N−Ni)/Å^{-1}		
fixed surface	2.04393	
relaxed surface	3.44928	
D_e(N−Ni)/cm^{-1}		
fixed surface	6041.79	
relaxed surface	4975.63	
r_e(N−Ni)/Å [b]	2.0097	-

[a] The N−H coupling data points were fitted separately to a linear coupling parameter. See text for details. [b] Value obtained from the DFT relaxation calculation.

TABLE 3: Accuracy of the N−H Potential Energy Point Fit to the Morse Function and to the Chebyshev Polynomial Expansion, for the Free NH_3 and NH_3 Adsorbed on the Atop Site of Ni(111), See Text

	RMS error/cm^{-1}	maximum deviation/cm^{-1}
atop Morse	112	1670
atop Chebyshev	12.4	10.2
free Morse	688	1300
free Chebyshev	7.7	9.6

at half-maximum (fwhm) line widths at 0 and 298 K are given in Table 4. The H−N−H bond angles used are from our DFT calculations and the values adopted are 107.41 and 110.07° for the free and adsorbed ammonia, respectively. For comparison, the harmonic vibrational wavenumbers for the N−H stretching modes are also given. They have been calculated using the coupling constants of the bilinear term in eq 3 and the second derivative of the most accurate analytic potential expression described above. It can be seen from Table 4 that the inclusion of anharmonicity significantly improves the agreement with experimental data.

The large range given for the N−Ni vibrational wavenumber reflects the finding that the shape of the N−Ni potential energy curve depends on whether the Ni surface is allowed to relax or not. The upper value of 519.5 cm^{-1} corresponds to the relaxed-surface case and the lower value of 307.9 to cm^{-1} to the fixed-surface case. It should be noted that besides the choice of the potential energy curve, the definition of the reduced mass of the N−Ni oscillator is also somewhat ambiguous. Should the oscillator be considered as an isolated $NiNH_3$ molecule, with a reduced mass of 13.2001 u, or as a NH_3 molecule vibrating against a solid surface of near-infinite mass, with a reduced mass of 17.0302 u? We attempted to resolve the problem in a physically reasonable manner by using the value 13.2001 u for the relaxed-surface case and the value 17.0302 u for the fixed-surface case. We found that the choice of the reduced mass affects the N−Ni vibrational wavenumber by ca. 40 cm^{-1}.

The large difference between the relaxed- and fixed-surface wavenumbers can be understood by noticing that our relaxation calculations do not account for the dynamic aspects of the vibrational motion and therefore lead to unreasonably large amplitudes for the oscillation of the Ni atoms. It was observed that especially the Ni atom closest to the ammonia molecule shifted significantly during the relaxation. For example, when the ammonia molecule was moved 0.5 Å toward the surface, the closest Ni atom retreated inward by over 0.3 Å. This might be physically unreasonable: since the ammonia molecule is much lighter than the nickel atom (not to mention the entire surface atom layer), the nickel atom should move much less. The real N−H vibrational wavenumber probably lies between the wavenumbers obtained from the relaxed- and fixed-surface potential energy curves, but considerably closer to the latter.

As our model accounts for the stretching vibrations only, and disregards the effect of all bending vibrations and nonperpendicular surface−adsorbate motions, it was not expected that calculated wavenumbers for both free ammonia and NH_3 bound to the surface to match the experimentally observed values perfectly. The precision of the density functional framework is also not sufficient to achieve high accuracy of calculated potential energy profiles. Instead, we are going to analyze the relative values, in particular, the changes in the N−H stretching wavenumbers of ammonia upon adsorption on the Ni(111) surface. The differences between calculated and experimental values for the red shifts caused by adsorption are on the order of 10 cm^{-1} for both N−H stretching fundamentals: 98 vs 86 cm^{-1} for the A_1 stretch and 90 vs 84 cm^{-1} for the E stretch. It should be noted that the experimental value for the E red shift is based on data by Fisher et al.,[11] with a resolution of 65 cm^{-1}, whereas the experimental value for the A_1 red shift is based on data by Xu et al.,[14] with a resolution of 4 cm^{-1}. Given that the line widths, as described below, are probably large, the agreement between calculated and experimental results is good. It also worth noticing that the red shifts calculated by the harmonic model are about 25−30 cm^{-1} lower than the experimental values. Thus, scaling the harmonic wavenumbers with one constant factor does not reproduce accurately the observed shifts.

The N−Ni stretching vibration has not been observed experimentally for a Ni(111) surface. This has been explained[11] by attenuation of the dynamic dipole of ammonia at the absorption site, although this was then thought to be the fcc hollow. The corresponding value for the Ni(110) surface has been given as alternatively 570 cm^{-1} (ref 11) and 450 cm^{-1} (ref 32). Our calculated wavenumber range of 307.9−519.5 cm^{-1} thus seems to be somewhat too low, especially when the real value is expected to be closer to the lower end of the range. Unfortunately, the lack of experimental data, and the ambiguities concerning the N−Ni potential energy curve described earlier, preclude further analysis.

3.4. N-H Stretching Vibration Line Widths. Our treatment of the N−H peak broadening is based on the observation that the N−H vibration is more rapid than the N−Ni vibration. Thus, we made an adiabatic approximation that the N−Ni distance is fixed for the classical period of the N−H vibration. An experimentally measured N−H stretching vibrational transition peak contains contributions from several N−H oscillators, each vibrating in a slightly different chemical environment due to different momentary N−Ni bond lengths. As a result, the measured N−H peak is broadened, the precise shape and width of the N−H spectral peak is observed depending on the N−Ni vibrational wave function, $\psi_{vib}(\Delta r_{N-Ni})$. The number of ammonia molecules at any given time that are at a distance Δr from the Ni surface is proportional to $[\psi_{vib}(\Delta r)]^2$.

TABLE 4: Calculated Fundamental Vibrational Transitions and the First Three Overtones for Stretching Wavenumbers in Isolated NH_3 and NH_3 Adsorbed on the Atop Site of Ni(111) and the N−H Peak Broadening Due to the N−Ni Vibration[j]

		NH_3		NH_3@Ni(111)		$\Delta\nu$ (ads)		fwhm broadening	
local[a]	sym	calc	obs	calc	obs	calc	obs	0 K	298 K
ω(100)[b]	A_1	3419.8		3359.5		60.3			
ω(100)[b]	E	3564.1		3512.3		51.8			
ν(100)	A_1	3278.4	3336.6[c]	3180.8	3251[d]	97.6	85.6	55	69
ν(100)	E	3415.4	3443.8[c]	3325.3	3360[e]	90.1	83.8	57	71
ν(200)	A_1	6492.1	6606.0[f]	6278.3		213.8		125	156
ν(200)	E	6581.1	6609.2[f]	6364.5		216.6		132	164
ν(110)	A_1	6749.6	6797.0[f]	6554.1		195.5			
ν(110)	E	6802.2	6850.5[f]	6618.2		184.0			
ν(300)	A_1	9617.3	9689.8[f]	9245.9		371.4			
ν(300)	E	9654.5	-	9273.7					
ν(N−Ni)				307.9−519.5[h]	570[g]				
					450[i]				

[a] Local mode assignment. [b] Harmonic wavenumbers. [c] Reference 37. [d] Reference 14. [e] Reference 11. [f] Reference 38. [g] NH_3 adsorbed on the Ni(110) surface. Reference 11. [h] Uncertainty due to the choice of surface relaxation and the N−Ni reduced mass, see text. [i] NH_3 adsorbed on the Ni(110) surface. Reference 32. [j] See text for further details. All energies are in cm^{-1}.

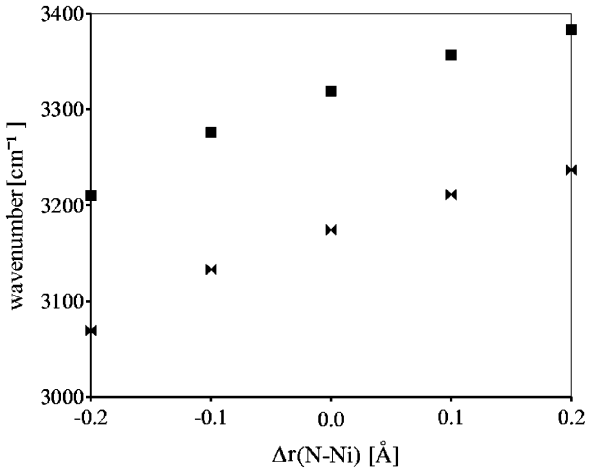

Figure 3. Dependence of the calculated fundamental wavenumbers of A_1 and E (solid squares) symmetry on the variation of the r(Ni−N) distance.

Since the A_1 and E stretching fundamentals and overtones were found to depend almost linearly on the N−Ni separation (see Figure 3 for the fundamentals) over the calculated range, the wavenumbers can be represented by the expression

$$\nu_{N-H} = m\,\Delta r_{N-Ni} + \nu_0 \qquad (4)$$

where m is a parameter and ν_0 is the wavenumber of the N−H stretching vibration at the N−Ni equilibrium distance. It should be noted that earlier studies on similar phenomena have assumed a quadratic dependence.[29] Through eq 4, ψ_{vib} can be expressed as a function of the vibrational wavenumbers. The number of N−H oscillators emitting or absorbing radiation at a certain wavenumber ν_{N-H} is then proportional to $[\psi_{vib}((\nu_{N-H} - \nu_0)/m)]^2$. To a reasonable approximation, ψ_{vib} can be assumed to be a linear combination of the Morse oscillator eigenfuctions,[33] the coefficients of the terms depending on the temperature according to the Boltzmann distribution, with any single oscillator in one eigenstate, and the probability of the eigenstate given by the Boltzmann factor.

The N−H stretching vibrational wavenumbers were fitted to eq 4. The obtained parameters, together with the root-mean-square (RMS) errors of the fits, are given in Table 5. These values, together with the Morse parameters for the N−Ni oscillator, were used to plot curves of $[\psi_{vib}((\nu_{N-H} - \nu_0)/m)]^2$ at different temperatures. Only the $\upsilon = 0-2$ contributions were included as the populations of higher energy states were negligible at room temperature. From these curves, the fwhm of the fundamental and first overtone transition peaks could be calculated.

TABLE 5: Numerical Values of the Parameters and RMS Errors of the Fits of the N−H Stretching Fundamental and First Overtone Wavenumbers to the N−Ni Distance at the Atop Site, Using the Fixed-Surface N−Ni Potential Energy Curve, See Text

local[a]	sym	ν_0/cm^{-1}	m/(cm^{-1}/Å)	RMS error/cm^{-1}
ν(100)	A_1	3164.93	413.50	12.8
ν(100)	E	3308.81	427.42	13.2
ν(200)	A_1	6237.04	937.94	28.8
ν(200)	E	6391.32	991.44	29.7

[a] Local mode assignment.

It should be noted that all broadening parameters and values refer to the "fixed-surface" N−Ni potential energy curve, which we assume to be more realistic due to reasons described above. The fwhm line widths were increased by around 20% when the "relaxed-surface" was adopted. The RMS errors of the various numerical fits involved in the process affect the broadening values by less than 5%.

There are few experimental data for NH_3 vibrational line widths on metal surfaces to compare our calculations with. The widths of the spectral lines presented by Fisher et al.[11] for the NH_3−Ni system are of the same order of magnitude as our calculated line widths, but the resolution of their EEL apparatus was 65 cm^{-1}. Therefore, no firm conclusions can be drawn. The A_1 stretching fundamental line width in the spectra presented by Xu et al.[14] is on the order of 30 cm^{-1}, with a resolution of 4 cm^{-1}, but the signal-to-noise-ratio of the A_1 peak is low. Line widths of the NH_3 stretching vibrations measured on Pt are also smaller than those calculated here, but of the same order of magnitude.[34]

To test the accuracy of the broadening model, the line width of the stretching vibration for CO adsorbed at the hcp site of the Ni(111) surface was computed. The energy cutoff for this calculation was 500 eV. All other parameters were kept at the values given in section 2.1. The broadening calculations for CO were carried out in the same way as described for NH_3 in section 2.2., except that the vibrational wavenumbers could be directly calculated from the fitted Morse parameters using an analytic formula, as there was only one oscillator to consider. The fwhm line width for the fundamental was determined to be 43 cm^{-1} at 0 K and 57 cm^{-1} at 298 K. This is large compared to the experimentally measured[29] line widths of around 10 cm^{-1} at

low temperatures. However, the experiment has been performed at high coverages, at which CO occupies bridge and atop sites, in which case the broadening is expected to be smaller than for 3-fold sites such as hcp, as described by Hoffman in ref 30. Unfortunately, there are no data for the broadening of the C−O vibration at Ni(111) surfaces at low coverage. For CO adsorbed at the Ni(110) surface at low coverages and at a temperature of 85 K, line widths on the order of 40 cm^{-1} have been measured.[35] For CO adsorbed at Pd(111) surfaces at low coverage, line widths of around 40 cm^{-1} have been determined[36] with an HREELS apparatus. Compared to these observations, our broadening values are somewhat large, but not unreasonable.

Although the absolute values for the fwhm broadening of both the N−H and C−O stretching vibrations are probably too large, our model correctly reproduces the qualitative experimental result that the N−H line widths are greater than the C−O line widths. This is remarkable, given that the much larger red shift (around 270 cm^{-1}, based on data from ref 29) of the C−O vibration upon adsorption would indicate a greater coupling between the metal−molecule and internal vibrations and could thus be expected to cause a greater line width using our model.

The difference between the calculated and measured line widths may be caused by the adiabatic approximation. As explained above, we calculated the intramolecular stretching potential energy curve at each molecule−metal distance. It is possible that the adiabatic approximation overestimates the contribution of the extreme displacements to the line width.

Accurate calculations of the line widths might also be thought to require the inclusion of the dependence of the HNH angle on the N−Ni bond length. This was studied by relaxing the hydrogen atoms while keeping all other atoms fixed in the positions corresponding to the points ±0.2 Å in the r(N−Ni) scan. For the compressed configuration, the equilibrium angle decreased by 0.48 degrees, and the bond length increased by 0.0025 Å, as the H atoms moved away from the Ni surface. For the stretched configuration, the angle increased by 0.31 degrees and the bond length decreased by 0.0019 Å. These changes in the geometry affect the kinetic energy coupling between the N−H oscillators and thus the N−H stretching vibrational term values. However, these contribute only about 1−2 cm^{-1} to the line widths in the case of the fundamentals and can be ignored. Another possibility is the contribution of the hot bands of the low wavenumber soft NH_3−Ni frustrated rotation bending modes, as a significant fraction of the NH_3−Ni bending oscillators could be in excited states at, for example, room temperature. The influence of this on the N−H stretching line widths and shapes may be significant.

Conclusion

Our calculations indicate that, in agreement with experimental results, the atop site is the most favorable for adsorption of NH_3 on the Ni(111) surface, with little azimuthal ordering of the adsorbed molecules. Further calculations show that the difference in adsorption energies between 0.25 and 0.11 ML coverages is caused by surface-mediated repulsive NH_3−NH_3 interactions. We also observe that NH_3 adsorption energies and geometries, along with the vibrational red shifts caused by adsorption, are well replicated with DFT methods. The results calculated with our anharmonic potential model show significant improvement over a simple harmonic analysis. Furthermore, we have provided a functioning method for using DFT potential energy data to calculate vibrational line widths caused by the coupling of intermolecular vibrations to molecule-surface vibrations.

Acknowledgment. M.B. acknowledges support of the EEC under the RTN Program 5 (Contract No. HPRN-CT-1999-00005). We thank CSC Scientific Computing Ltd. From Espoo for providing computer time. L.H. is grateful to the Academy of Finland for financial support. We thank Teija Kangas from the University of Oulu for calculations concerning the CO molecules.

References and Notes

(1) Eichler, A. Ph.D. Dissertation Small Molecules at Metallic Surfaces. Available online at http://cms.mpi.univie.ac.at/eichler/

(2) Zumdahl, S. S. *Chemistry*, 4th ed.; Houghton Mifflin Company: New York, 1997.

(3) Halonen, L.; Bernasek, S. L.; Nesbitt, D. J. *J. Chem. Phys.* **2001**, *115*, 5611.

(4) Beck, R. D.; Maroni, P.; Papageorgopoulos, D. C.; Dang, T. T.; Schmid, M. P.; Rizzo, T. T. *Science* **2003**, *302*, 98.

(5) Seabury, C. W.; Rhodin, T. N.; Purtell, R. J.; Merrill, R. P. *Surf. Sci.* **1980**, *93*, 117.

(6) Netzer, F. P.; Madey, T. E. *Phys. Rev. Lett.* **1981**, *47*, 928.

(7) Madey, T. E.; Houston, J. E.; Rhodin, T. N.; Seabury, C. W. *J. Vac. Sci. Technol.* **1981**, *18*, 476.

(8) Kang, W. M.; Li, C. H.; Tong, S. Y.; Seabury, C. W.; Jacobi, K.; Rhodin, T. N.; Purtell, R. J.; Merrill, R. P. *Phys. Rev. Lett.* **1981**, *47*, 931.

(9) Seabury, C. W.; Rhodin, T. N.; Purtell, R. J.; Merrill, R. P. J. *Vac. Sci. Technol.* **1981**, *18*, 602.

(10) Netzer, F. P.; Madey, T. E. *Surf. Sci.* **1982**, *119*, 422.

(11) Fisher, G. B.; Mitchell, G. E. *J. Electron Spectrosc. Relat. Phenom.* **1983**, *29*, 253.

(12) Bozso, F.; Arias, J. M.; Hanrahan, C. P.; Yates, J. T., Jr.; Metiu, H.; Martin, R. M. *Surf. Sci.* **1984**, *138*, 488.

(13) Dresser, M. J.; Lanzillotto, A.-M.; Alvey, M. D.; Yates, J. T., Jr. *Surf. Sci.* **1987**, *191*, 1.

(14) Xu, Z.; Hanley, L.; Yates, J. T., Jr. *J. Chem. Phys.* **1992**, *96*, 1621.

(15) Schindler, K.-M.; Fritzsche, V.; Asensio, M. C.; Gardner, P.; Ricken, D. E.; Robinson, A. W.; Bradshaw, A. M.; Woodruff, D. P.; Conesa, J. C.; González-Elipe, A. R. *Phys. Rev. B* **1992**, *46*, 4836.

(16) Redondo, A.; Zeiri, Y.; Low, J. L.; Goddard, W. A. *J. Chem. Phys.* **1983**, *79*, 6410.

(17) Chattopadhyay, A.; Yang, H.; Whitten, J. L. *J. Phys. Chem.* **1990**, *94*, 6379.

(18) VASP, Vienna Ab Initio Simulation Package written by G. Kresse and J. Furthmüller; Kresse, G.; Hafner, J. *Phys. Rev. B* **1993**, *47*, 558. Kresse, G.; Furthmüller, J. *Comput. Mater. Sci.* **1996**, *6*, 15. Kresse, G.; Furthmüller, J. *Phys. Rev. B* **1993**, *54*, 11169.

(19) Moroni, E. G.; Kresse, G.; Hafner, J.; Furthmüller, J. *Phys. Rev. B* **1997**, *56*, 15629.

(20) Hafner, J. *J. Mol. Struct.* **2003**, *651*−*653*, 3.

(21) Tuckerman, M. E.; Ungar, P. J.; von Rosenvinge, T.; Klein, M. L. *J. Phys. Chem.* **1996**, *100*, 12878.

(22) Rajamäki, T.; Kallay, M.; Noga, J.; Valiron, P.; Halonen, L. *Mol. Phys.* **2004**, *102*, 2297.

(23) Morse, P. M. *Phys. Rev.* **1929**, *34*, 57.

(24) Pesonen, J.; Miani, A.; Halonen, L. *J. Chem. Phys.* **2001**, *115*, 1243.

(25) Child, M. S.; Halonen, L. *Adv. Chem. Phys.* **1984**, *57*, 1. Halonen, L. *Adv. Chem. Phys.* **1998**, *104*, 41.

(26) Halonen, L.; Child, M. S. *J. Chem. Phys.* **1983**, *79*, 4354.

(27) Kauppi, E.; Halonen, L. *J. Phys. Chem.* **1990**, *94*, 5779.

(28) Persson, B. N. J.; Persson, M. *Solid State Commun.* **1980**, *36*, 175.

(29) Persson, B. N. J.; Rydberg, R. *Phys. Rev. B* **1985**, *32*, 3586.

(30) Hoffman, F. M. *Surf. Sci. Rep.* **1983**, *3*, 107.

(31) Honkala, K.; Pirilä, P.; Laasonen, K. *Phys. Rev. Lett.* **2001**, *86*, 5942.

(32) Bassignana, I. C.; Wagemann, K.; Küppers, J.; Ertl, G. *Surf. Sci.* **1986**, *175*, 22.

(33) Nieto, M. M.; Simmons, L. M., Jr. *Phys. Rev. A* **1978**, *19*, 438.

(34) Villegas, I.; Weaver, M. J. *Surf. Sci.* **1996**, *367*, 162.

(35) Grossmann, A.; Erley, W.; Ibach, H. *Surf. Sci.* **1996**, *355*, L331.

(36) Surnev, S.; Sock, M.; Ramsey, M. G.; Netzer, F. P.; Wiklund, M.; Borg, M.; Andersen, J. N. *Surf. Sci.* **2000**, *470*, 171.

(37) Spirko, V.; Kraemer, W. P. *J. Mol. Spectrosc.* **1989**, *133*, 331.

(38) Coy, S. L. Lehmann, K. K. *Spectrochim. Acta A* **1989**, *45*, 47.